Optimization of a *Plasmodium falciparum* circumsporozoite protein repeat vaccine using the tobacco mosaic virus platform

Mark D. Langowski[a,1], Farhat A. Khan[a,1], Alexis A. Bitzer[a], Christopher J. Genito[a], Andrew J. Schrader[b], Monica L. Martin[b], Kimberly Soto[a], Xiaoyan Zou[c], Sri Hadiwidjojo[c], Zoltan Beck[d,e], Gary R. Matyas[e], Merricka C. Livingstone[a], Adrian H. Batchelor[a], and Sheetij Dutta[a,2]

[a]Malaria Vaccine Branch, Walter Reed Army Institute of Research, Silver Spring, MD 20910; [b]Division of Veterinary Medicine, Walter Reed Army Institute of Research, Silver Spring, MD 20910; [c]Malaria Department, Naval Medical Research Center, Silver Spring, MD 20910; [d]Henry M Jackson Foundation for the Advancement of Military Medicine, Rockville, MD 20817; and [e]Military HIV Research Program, Walter Reed Army Institute of Research, Silver Spring, MD 20910

Edited by David Baker, University of Washington, Seattle, WA, and approved December 27, 2019 (received for review July 15, 2019)

Plasmodium falciparum **vaccine RTS,S/AS01 is based on the major NPNA repeat and the C-terminal region of the circumsporozoite protein (CSP). RTS,S-induced NPNA-specific antibody titer and avidity have been associated with high-level protection in naïve subjects, but efficacy and longevity in target populations is relatively low. In an effort to improve upon RTS,S, a minimal repeat-only, epitope-focused, protective, malaria vaccine was designed. Repeat antigen copy number and flexibility was optimized using the tobacco mosaic virus (TMV) display platform. Comparing antigenicity of TMV displaying 3 to 20 copies of NPNA revealed that low copy number can reduce the abundance of low-affinity monoclonal antibody (mAb) epitopes while retaining high-affinity mAb epitopes. TMV presentation improved titer and avidity of repeat-specific Abs compared to a nearly full-length protein vaccine (FL-CSP). NPNAx5 antigen displayed as a loop on the TMV particle was found to be most optimal and its efficacy could be further augmented by combination with a human-use adjuvant ALFQ that contains immune-stimulators. These data were confirmed in rhesus macaques where a low dose of TMV-NPNAx5 elicited Abs that persisted at functional levels for up to 11 mo. We show here a complex association between NPNA copy number, flexibility, antigenicity, immunogenicity, and efficacy of CSP-based vaccines. We hypothesize that designing minimal epitope CSP vaccines could confer better and more durable protection against malaria. Preclinical data presented here supports the evaluation of TMV-NPNAx5/ALFQ in human trials.**

vaccines | antigenicity | immunogenicity | malaria | CSP

Malaria caused by *Plasmodium falciparum* is transmitted to humans through the bite of an infected female *Anopheles* mosquito. In 2017 alone, 219 million infections and 435,000 deaths world-wide were attributed to malaria (1). The *Plasmodium* sporozoite stage, transmitted by a mosquito, is covered primarily by the circumsporozoite protein (CSP) that consists of an N-terminal region that is highly conserved, followed by a repetitive region containing a junctional region and 25 to 42 copies of NPNA repeats, which is followed by a cysteine-rich C-terminal region (2, 3). The C-terminal region is polymorphic and the N-terminal region may not be exposed during sporozoite transit from the mosquito to man for antibody (Ab) binding (4–7). Abs against CSP repeats are a critical component of protection induced by the most advanced malaria vaccine candidate, RTS,S/AS01 (Mosquirix, GlaxoSmithKline) (8, 9). RTS,S is a recombinant CSP vaccine, containing 19 copies of the major NPNA repeats and the C-terminal region of CSP fused to the N terminal of the hepatitis B *S* antigen particle and is formulated with a potent adjuvant AS01 (10).

The RTS,S/AS01 vaccine induced protection against diverse parasites in the field is low and it wanes within a few months (6, 11–13). Since it was first reported in 1995 (14), no further attempts were made to improve the design of RTS,S. Second-generation CSP vaccines are under development, including immunogens like the Walter Reed Army Institute of Research's nearly full-length CSP (FL-CSP) (15–17), hepatitis B particles with higher CSP epitope density than RTS,S (18), epitope broadened vaccines (19, 20), or vaccines based on novel viral capsids or designed de novo (21–26). All of these reports generally agree that the major poly-NPNA repeat is the most important target of protective Abs and one report suggested that a higher repeat copy number could improve Ab-mediated complement fixation (27).

Several lines of evidence suggest that it may be possible to rationally improve upon the efficacy of CSP-based vaccines. For example, fractionating and delaying the third RTS,S dose

Significance

RTS,S/AS01 is a circumsporozoite protein (CSP)-based malaria vaccine that confers partial protection against malaria in endemic areas. Recent reports have elucidated structures of monoclonal antibodies that bind to the central (NPNA) repeat region of CSP and that inhibit parasite invasion. Antigen configuration and copy number of CSP repeats displayed on a tobacco mosaic virus (TMV) particle platform were studied. A TMV vaccine containing CSP repeats displayed as a loop induced 10× better antibody titer than a nearly full-length CSP in mice. In rhesus model, this translated to a 5× improvement in titer. Rhesus antibodies potently inhibited parasite invasion up to 11 mo after vaccination. An optimized epitope-focused, repeat-only CSP vaccine may be sufficient or better than the existing CSP vaccines.

Author contributions: A.H.B. and S.D. designed research; M.D.L., F.A.K., A.A.B., C.J.G., A.J.S., M.L.M., K.S., X.Z., S.H., M.C.L., A.H.B., and S.D. performed research; Z.B., G.R.M., and S.D. contributed new reagents/analytic tools; M.D.L., A.A.B., C.J.G., A.H.B., and S.D. analyzed data; and M.D.L., A.H.B., and S.D. wrote the paper.

Competing interest statement: M.D.L., F.A.K., A.H.B., and S.D. have filed a patent on the tobacco mosaic virus (TMV)-based malaria vaccine described herein.

This article is a PNAS Direct Submission.

Data deposition: The data reported in this paper have been deposited in the Figshare database at https://figshare.com/projects/Optimization_of_a_Plasmodium_Falciparum_Circumsporozoite_Protein_Repeat_Vaccine_using_the_Tobacco_Mosaic_Virus_Platform/73019.

[1]M.D.L. and F.A.K. contributed equally to this work.

[2]To whom correspondence may be addressed. Email: sheetij.dutta.civ@mail.mil.

This article contains supporting information online at https://www.pnas.org/lookup/suppl/doi:10.1073/pnas.1911792117/-/DCSupplemental.

First published January 27, 2020.

improved efficacy that was associated with an increased Ig gene diversity and higher Ab avidity (28). Monoclonal antibodies (mAbs) isolated from this more protective RTS,S regimen mapped inhibitory Abs to the central NPNA repeat region. For example, mAb 317 blocked sporozoite invasion into hepatocytes and it bound to poly-NPNA peptide with nanomolar affinity (29). Epitopes upstream of the major CSP repeats (regions not included in RTS,S) also induce inhibitory mAbs following exposure to whole sporozoites (30, 31). Many of these human CSP mAbs are now being considered as tools for malaria control by passive transfer. Although mAbs may confer short-term protection, cost–benefit analyses may reveal hurdles in the mass administration of mAbs to infants and pregnant women (32, 33). Structural data emerging from mAbs has, however, revealed vulnerabilities on parasite antigens that can now be utilized to design the next-generation malaria vaccines that focus the host response to a narrow range of protective epitopes, recapitulating the protective responses achieved by passive transfer of mAbs (34, 35). An example of this approach was utilized for F glycoprotein of respiratory syncytial virus (RSV), where neutralizing mAbs revealed the cause of vaccine failure (36), and then were used to allow improved targeting of neutralization-sensitive sites in a second-generation vaccine (37). The structural data that has emerged from CSP mAbs could perhaps also be used in a similar manner to probe improvements on CSP vaccines.

To probe the conformational states of poly-NPNA, human mAbs that bind to distinct conformations of poly-NPNA and have different affinities can be used. mAb 580 was isolated from a naturally exposed individual and shown to bind to an elongated conformation of $(NPNA)_2$ peptide (35) (*SI Appendix*, Fig. S1*A*). mAb 317 was isolated from an RTS,S vaccinee and shown to bind to a "curved" conformation of $(NPNA)_3$ peptide (29) (*SI Appendix*, Fig. S1*B*). mAb CIS43 was isolated from an irradiated sporozoite vaccinee, and it preferentially binds to the N-terminal NPNA repeat junction region and to $(NPNA)_2$ in a curved conformation (31) (*SI Appendix*, Fig. S1 *C* and *D*). mAb 317 and CIS43 affinity constants are in the low nanomolar range, compared to micromolar affinity reported for mAb 580 (29, 31, 35).

Flexibility has been shown to influence the immunogenicity of epitopes. An inherently disordered, repeat region containing malaria antigen MSP-2, showed that the most flexible regions were minimally immunogenic compared to ordered regions (38). CSP is also an unstructured repeat containing antigen. mAb epitopes reveal that the repeat region of CSP harbors a myriad of short hydrogen-bonded epitopes (39, 40) that are bound by both low- and high-affinity Abs. Since the long CSP repeat region contains many conformations of NPNA in equilibrium, reducing copy number and adding structural constraints could be a way to reduce antigenic promiscuity and conformational disorder. To test this, different lengths of NPNA peptides were displayed on a virus-like particle (VLP). We utilized an open source particle technology based on the tobacco mosaic virus (TMV) VLP for this design effort. TMV under physiological conditions assembles into an 18-nm disk that can also further assemble into rod shaped VLPs of up to 300 nm in size (41). The TMV size range and, its repetitive, symmetric, and high-density display of epitopes make them highly attractive for antigen presentation and induction of high titer antibodies (42).

We have previously shown that FL-CSP administered with a molecular adjuvant, ALFQ (army liposome formulation containing QS21), meets the historical immunogenicity benchmark of RTS,S/AS01 in humans (43, 44). Significant superiority over this FL-CSP/ALFQ formulation is a progression criterion for down-selection of the next generation of CSP vaccines. A series of TMV-based NPNA repeat vaccines were tested here in mice revealing that a short NPNAx5 antigen displayed on a constrained loop showed diminished binding to a low-affinity mAb while still binding efficiently to a higher-affinity mAb. This TMV-NPNAx5 vaccine exceeded the immunogenicity and efficacy of our first-generation FL-CSP vaccine in mice. The superiority of TMV-NPNAx5/ALFQ over FL-CSP/ALFQ was replicated in rhesus, supporting the progression of this next-generation CSP vaccine to human trials.

General Methods

For detailed methods, please refer to *SI Appendix*.

Vaccines. Mapping of protective regions of CSP was performed using *Escherichia coli*-derived GST fusion protein vaccines containing the N-terminal (NT-CSP; residues Y_{26}-P_{104}), repeat (Repeat-CSP; residues L_{94}-N_{284}), and C-terminal region (CT-CSP; residues K_{274}-L_{387}) of CSP (*SI Appendix*, Fig. S2). Repeat antigenicity and immunogenicity was optimized using TMV capsid proteins produced in *E. coli*. TMV particles displaying NPNAx3, -x4, -x5, -x7, -x10, or -x20 on an exposed loop (TMV-Loop) were produced. The NPNAx5 also displayed on the N terminal (TMV-NT) and C terminal (TMV-CT) of the TMV particle. Particles were characterized for purity, identity, endotoxin content, and presence of TMV-like particles was determined by electron microscopy.

mAbs and Antigenicity. Fab sequences of mAb 580 (35), mAb 317 (29), and mAb CIS43 (31) were grafted onto human IgG1 Fc and the resulting full-length IgGs were produced in HEK293 cells. An enzyme linked immunosorbent assay (ELISA) was conducted with TMV repeat particles or FL-CSP coated on plates (100 ng per well) and concentration of mAb that resulted in OD = 1 was determined as a measure of mAb-binding potency.

Mouse Immunogenicity and Challenge. C57BL/6 (H-2b) mice ($n = 10$ per group) were used for serological comparisons. Functionality of antisera in mice was determined by challenge with *Plasmodium berghei* FL-CSP transgenic sporozoites (45). Protection was defined as an absence of parasites in the mouse blood (46). Vaccines were formulated in the oil-in-water adjuvant, AddaVax (InvivoGen) or in the ALFQ that contains the immune-modulators, 3D-PHAD and QS21 (43). Mice were vaccinated three times with 1.25 to 2.5 μg protein (kept constant within an experiment) at 3-wk intervals, intramuscularly in alternating thigh muscles. Serological assays used $(NPNA)_6$ peptide, FL-CSP protein, TMV particles with NPNAx3, and NPNAx20 repeats as plate antigens. ELISA end-point titer was defined as the serum dilution that gave an $OD_{415} = 1$. An IgG2c/IgG1 subclass ELISA was also performed.

Rhesus Immunogenicity. Rhesus monkeys of Indian origin ($n = 6$ per group) were vaccinated three times at 3-wk intervals, with 20 μg TMV-NPNAx5, 40 μg TMV-NPNAx5, or 40 μg FL-CSP; all antigens were adjuvanted with 1 mL ALFQ. Three doses were given on days 0, 28, and 60, in alternating thigh muscles. Monkeys were bled 2 wk after each vaccination and then monthly up to 6 mo after the last vaccine dose. A subset of monkeys, the 20 μg TMV-NPNAx5 ($n = 3$) and 40 μg TMV-NPNAx5 ($n = 2$) group, and for the 40 μg FL-CSP group ($n = 2$), were bled again at week 47 after the third dose to access durability. In another study, rhesus of Chinese origin were vaccinated three times with 40 μg TMV-NPNAx5 ($n = 6$), 40 μg TMV-NPNAx20 ($n = 4$), or 40 μg FL-CSP ($n = 6$) and sera was analyzed 2 wk after third dose. Sera were analyzed for function using an inhibition of liver stage development assay (ILSDA) (47). Repeat-specific ELISA and avidity assays were performed by the International Malaria Serology Reference Center using human ELISA methodology, as previously described for the RTS,S/AS01, MAL071 clinical trial (28).

Ethics Statement. Animal procedures were conducted in compliance with the Animal Welfare Act and other federal statutes and regulations relating to animals and experiments involving animals, and adhere to principles stated in the *Guide for the Care and Use of Laboratory Animals*, National Research Council Publication, 2011 edition (48).

Results

Rationale for Repeat-Only CSP Vaccines. Regions of CSP that confer maximal protection in a transgenic mouse challenge model were mapped using subunit proteins produced in *E. coli* (*SI Appendix*, Figs. S2 and S3). The CSP-repeat region, C-terminal region, and FL-CSP Abs reacted with the sporozoite surface by immunofluorescence assay, but N-terminal Abs were nonreactive (*SI Appendix*, Fig. S3*B*). No ILSDA activity was observed for the C

terminal; Abs to the N terminal showed midlevel inhibition (~1 log reduction); and CSP repeat Abs showed the highest (~2 log) reduction in parasite mRNA burden (*SI Appendix*, Fig. S3*C*). While repeat region Abs had lower average avidity than the C-terminal Abs, sterile protection was only detected when vaccines contained the poly-NPNA CSP repeat region (*SI Appendix*, Fig. S3 *D* and *E*).

Repeat-Only TMV Vaccine Design. The N and C termini of the TMV capsid point outwards from an assembled TMV disk (Fig. 1*A*) and majority of previous vaccine design efforts have used these N and C termini to display epitopes (41, 49–52). Dedeo et al. (53) reported a "circular permutant" of TMV where the N and C termini were re-engineered to the inner pore and a short loop was placed to close the sequence gap. We used this circular permutant of TMV to display the NPNA repeats on the exposed loop (Fig. 1 *B* and *C*). TMV circular permutants displaying various NPNA copy numbers from NPNAx3 to NPNAx20 were designed and predicted tertiary structures [Rosetta Protein Prediction Server (54, 55); http://robetta.bakerlab.org] illustrated the expected increasing conformational complexity and flexibility at higher copy numbers (Fig. 2*A*). To determine the best location of the NPNAx5 antigen within the TMV monomer, we utilized the native fold of TMV to display NPNAx5 on the N terminus (TMV-NT) or the C terminus (TMV-CT). Overlaid predicted minimum energy structures illustrated that N- and C-terminal display on native TMV fold would also lead to increased antigen flexibility compared to the loop display (TMV-Loop) (Fig. 2*B*). TMV vaccine antigens were >95% pure, reactive to a repeat-specific mouse mAb 2A10 (56) (*SI Appendix*, Fig. S4), and they contained TMV-like disks and rods as visualized by electron microscopy (Fig. 2).

Antigenicity of TMV Vaccines. The ability of multiple CSP repeat-specific mAbs to bind to the TMV-NPNA constructs was determined. All three mAbs (580, CIS43, and 317) bound to FL-CSP was high potency (<10 ng/mL for OD = 1) (Fig. 3 *A* and *B*). Among the NPNAx3 to NPNAx20 TMV vaccines, mAb 580 potency positively associated with copy number (2.2 ng/mL for NPNAx3 to >1,049 ng/mL for NPNAx20; Spearman's correlation < 0.01). MAb 317 bound potently to all copy numbers (<7 ng/mL), with a slightly diminishing potency with increasing copy number (3 to 7 ng/mL) (Fig. 3*B*). MAb CIS43 also potently bound to all NPNA copy-number vaccines (<11 ng/mL), except NPNAx3 (476 ng/mL) (Fig. 3*B*). For NPNAx5 displayed on Loop, NT, or CT, the potency of mAbs 317 and CIS43 showed little difference (<10 ng/mL). However, mAb 580 potency for TMV-CT (139 ng/mL) was reproducibly ~threefold higher than TMV-Loop (541 ng/mL) (Fig. 3 *C* and *D* and *SI Appendix*, Fig. S5).

TMV Vaccines Were Superior to FL-CSP and Immunogenicity Increased Between NPNAx3 to NPNAx5. We sought to determine the effect of NPNA copy number on antibody quality and protective outcomes. TMV vaccines displaying NPNAx3, NPNAx4, NPNAx5, and FL-CSP (contains 19 copies of NPNA) were formulated in AddaVax adjuvant and used to vaccinate C57BL/6 mice (Fig. 4 *A*–*C*). NPNAx5 induced ≥twofold higher NPNA-specific titers than NPNAx4, NPNAx3, and FL-CSP vaccines (Fig. 4*A* and *SI Appendix*, Fig. S6*A*). Challenge with transgenic parasites showed no protection in the controls but the best protection was seen in NPNAx5 (66% of mice did not become infected) compared to NPNAx4 (60%), NPNAx3 (10%), and FL-CSP (20%) (Fig. 4*C*). NPNA peptide avidity was higher in the TMV vaccine groups compared to FL-CSP (Fig. 4 *B*, *Left*), but NPNAx3, NPNAx4, or NPNx5 group avidity did not differ (Fig. 4*B*). Distribution of protected (Fig. 4*A*, red symbols) and unprotected (Fig. 4*A*, black symbols) showed that >60% mice with high titer ($>10^4$) were protected compared to ~10% protection at lower titers.

TMV Display of NPNAx5 Was Optimal for High Titer and Avidity. The next mouse study sought to determine if a higher copy number than NPNAx5 further improved the vaccine. We tested TMV-NPNAx5, NPNAx7, NPNAx10, and NPNAx20 vaccines formulated in AddaVax (Fig. 4 *D*–*F*). TMV-NPNAx5 titer trended to be the higher than other groups, but the difference was not statistically significant (Fig. 4*D* and *SI Appendix*, Fig. S6*B*). All negative control mice were infected postchallenge, but similar levels of sterile protection were seen in all groups: NPNAx5 (60%), NPNAx7 (50%), NPNAx10 (60%), and NPNAx20 (60%) (Fig. 4*F*). Avidity measured using the NPNA peptide coat was similar, but when using the full-length protein as coat antigen, the TMV-NPNAx5 group had superior avidity to NPNAx20 (Fig. 4*E*). In summary, neither the titer nor the avidity improved above NPNAx5, and very high copy numbers (NPNAx20, FL-CSP) negatively impacted avidity in mice.

Reducing Antigen Flexibility Improved Titer and Avidity. We next sought to determine if the immunogenicity of the NPNA repeats could be improved by moving display of NPNA from the TMV-Loop to the TMV-NT or TMV-CT. The immunogenicity of NPNAx5 displayed as TMV-NT, -CT, and -Loop were compared to FL-CSP using AddaVax (Fig. 4 *G*–*I*). The Loop titer was significantly higher than NT, CT, and ~10-fold higher than FL-CSP (Fig. 4*G* and *SI Appendix*, Fig. S6*C*). Following challenge, all control mice were infected and protection was highest in the Loop (30%), compared to NT (10%), FL-CSP (10%), and CT (0%) groups (Fig. 4*I*). NPNA peptide and protein avidity for the Loop was higher than NT, CT, and FL-CSP (Fig. 4*H*), and TMV-CT

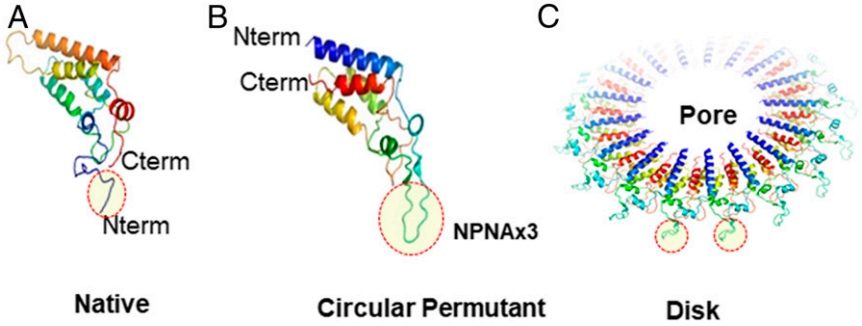

Fig. 1. Predicted TMV capsid structures. (*A*) The native fold of the TMV monomer displaying NPNAx3 (circled) at the N terminus. (*B*) Circular permutant of TMV, where the N and C termini have been repositioned to the pore and an exposed loop was used to display NPNAx3. (*C*) Model of a TMV disk showing the exposed loops with NPNAx3 (based on 3KML crystal structure). All structures were predicted using Rosetta prediction server and pictures generated using PyMOL software.

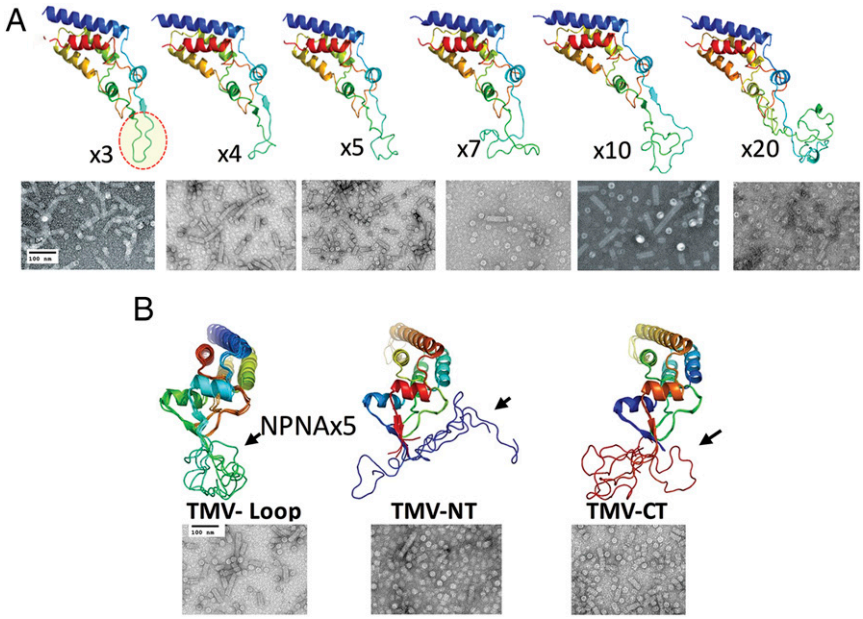

Fig. 2. Design and production of TMV particles. (*A*) Rosetta structure predictions showing poly-NPNA of various lengths on the exposed loop (NPNAx3 circled). (*B*) Overlaid, minimum energy structures of NPNAx5 antigen (arrows) on the exposed loop of the circular permutant (Loop) or on the N terminal (NT) and C terminal (CT) of the native TMV fold, as predicted by Rosetta protein prediction server. Shown below each structure is the electron micrograph (40,000×) of the respective vaccine preparation.

avidity was no different from FL-CSP. Protection was generally low in this experiment, but protected mice (Fig. 4 *G* and *H*, red symbols) clustered around higher titer and avidity points (Fig. 4 *G* and *H*). We concluded that NPNA displayed as a loop was superior to N- or C-terminal extensions.

Lowering Copy Number and Flexibility Pivoted Abs toward Constrained Conformations. In an ELISA, the ratio of reactivity to TMV NPNAx3 (representing constrained conformations) and TMV-NPNAx20 (representing flexible and constrained conformations) was determined (*SI Appendix*, Fig. S7). A caveat of this ELISA set-up is that it also captured TMV backbone antibodies. FL-CSP had the lowest NPNAx3/NPNAx20 OD_{415} ratio (Fig. 4 *J* and *K*). A proportional drop in constrained NPNA-specific Ab response was detected with increasing vaccine copy number (Fig. 4*J*). NPNAx3/NPNAx20 OD_{415} ratio for Loop was highest compared to NT, CT, and FL-CSP (Fig. 4*K* and *SI Appendix*, Fig. S7*B*). Thus, low copy number or tethering NPNA as a loop could augment the Ab response to the constrained conformations.

TMV-NPNAx5 Formulated in ALFQ Enhances Protection. To be highly efficacious, RTS,S required formulation in adjuvants containing the immune-stimulators QS21 and bacterial monophosporyl-lipid A (9). We next tested TMV-NPNAx5 in ALFQ, a liposomal adjuvant, containing similar immune-stimulators (43). Mice immunized with TMV-NPNAx5 and FL-CSP antigens in ALFQ showed 10× higher repeat-specific titers in the TMV-NPNAx5 group (Fig. 5*A* and *SI Appendix*, Fig. S6*D*). Transgenic parasite

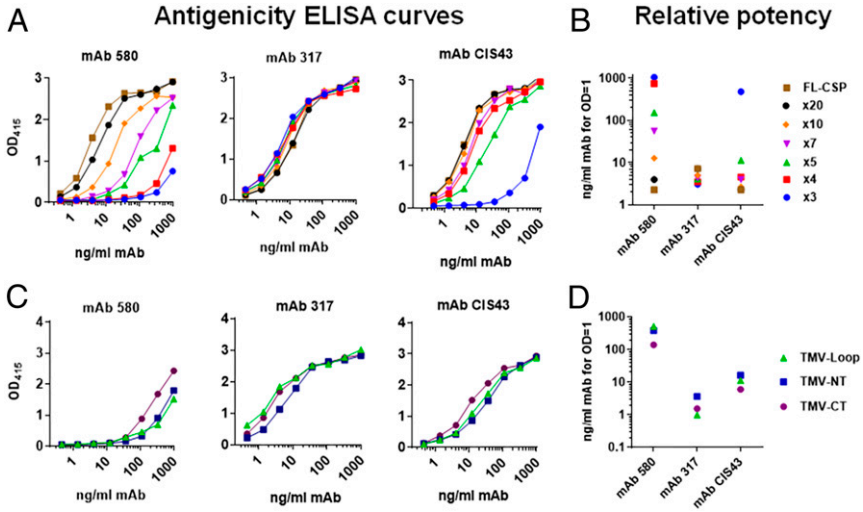

Fig. 3. (*A* and *C*) ELISA titration curves of mAb 580, mAb 317 and CIS43 against TMV antigens expressing various copy numbers of poly-NPNA or the NPNAx5 displayed on the Loop, NT, or CT of the TMV monomer. All antigens were coated at 100 ng/mL. (*B* and *D*) Relative potency (OD = 1 mAb concentration) for ELISA curves shown in *A* and *C*, respectively.

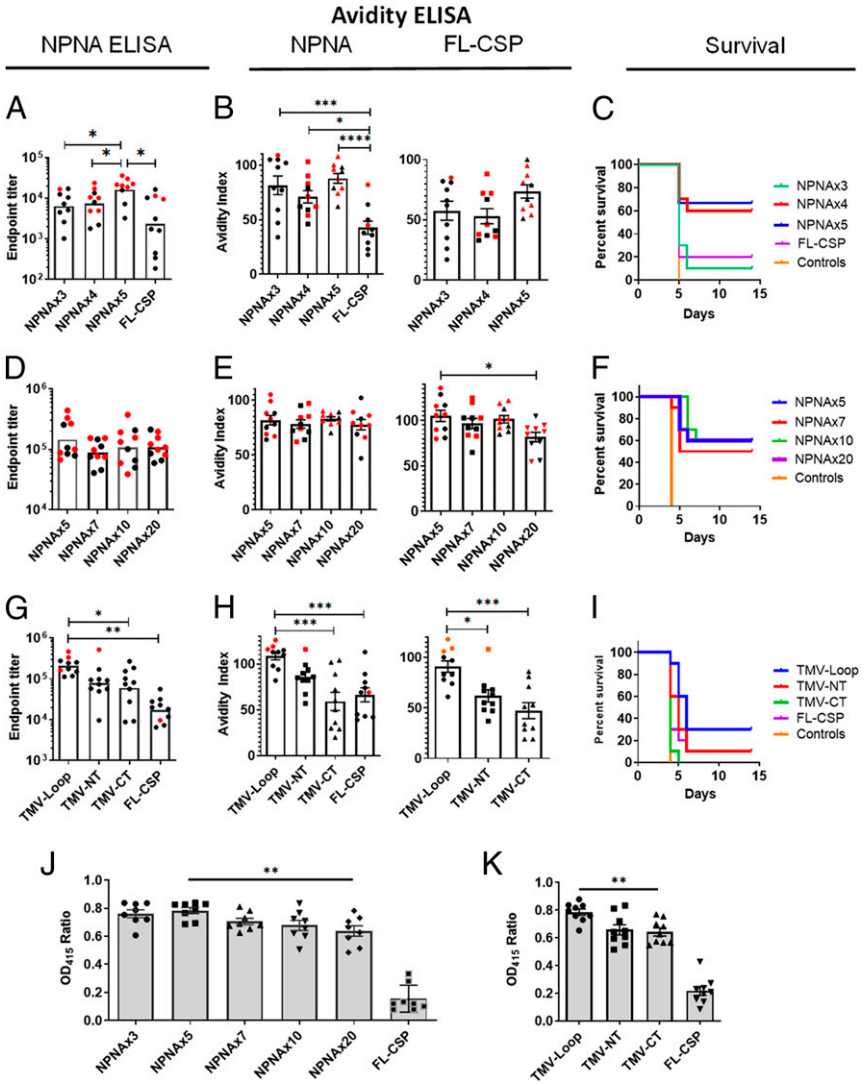

Fig. 4. Optimization of immunogenicity of TMV vaccines/AddaVax in C57BL/6 mouse challenge model. Mice (n = 10) were vaccinated thrice with 1.25 μg TMV-NPNAx3, -x4, -x5, or FL-CSP vaccines (*A–C*) or with 2.5 μg TMV-NPNAx5, -x7, -x10, and -x20 vaccines (*D–F*) or with 1.25 μg TMV-NPNAx5-Loop, -NT, -CT, or FL-CSP (*G–I*) using AddaVax adjuvant. All vaccines were given at 3-wk intervals ELISA and challenge was at 2 wk after the third dose. (*A*, *D*, and *G*) Geometric mean ELISA titer using $(NANP)_6$ peptide coat. (*B*, *E*, and *H*) Mean avidity index using either a repeat peptide coat (*Left*) or FL-CSP coat (*Right*). (*C*, *F*, and *I*) Survival curves of mice postchallenge. (*J* and *K*) Mean OD_{415} ratio for NPNAx3/NPNAx20 coated plates for mouse sera tested at 1:8,000 dilution. Error bars are ±SEM; red symbols are protected mice and asterisks indicate the level of statistical significance. ****$P < 0.0001$; ***$P < 0.001$; **$P < 0.01$; *$P < 0.05$.

challenge resulted in 100% protection in the TMV-NPNAx5 group compared to 20% protection in the FL-CSP group (Fisher's exact test: $P = 0.0007$) (*SI Appendix*, Fig. S5*C*). An avidity ELISA confirmed higher TMV-NPNAx5 avidity over FL-CSP (Fig. 5*B*). An ELISA using full-length protein or (NANP)x6 peptide showed that FL-CSP induced almost the same total CSP-specific Abs as TMV-NPNAx5; the major difference being the ∼1 log lower repeat-specific titers in FL-CSP vaccinated mice (Fig. 5*D*), thus demonstrating focusing of Abs to the repeat region using the TMV platform.

The original copy-number comparison study performed with Addavax adjuvant (Fig. 4 *D–F*) was repeated using ALFQ adjuvant (Fig. 5 *E–J*). The TMV-NPNAx5 group showed higher titers than NPNAx7, -x10, and -x20 vaccines (*SI Appendix*, Fig. S6*E*), and titer difference between NPNAx5 and NPNAx20 reached statistical significance in ALFQ (Fig. 5*E*). An avidity ELISA showed no difference between vaccines but a trend toward lower avidity in NPNAx20 was again noted (Fig. 5*F*). In all groups except NPNAx20 (90%), 100% protection was observed (Fig. 5*G*). Since most mice survived the first challenge, sera at 10 and 15 wk after the third dose were tested by ELISA and mice were rechallenged at week 15. Repeat titers dropped ∼fivefold across all TMV groups in 11 wk following the last dose, but titers plateaued in all groups by 15 wk (Fig. 5*H*). Rechallenge showed varying levels of partial protection: NPNAx5 (50%), NPNAx7 (50%), NPNAx10 (60%), and NPNAx20 (77%) (Fig. 5*I*). IgG2c Abs have been associated with higher protection in the mouse model (15) and a subclass ELISA (Fig. 5*J*) confirmed that ALFQ induced higher levels of IgG2c compared to Addavax adjuvanted vaccines (Fig. 4 *D–F*). A 10× immunological superiority of vaccines containing ∼five NPNA repeats over FL-CSP/ALFQ was observed. While TMV-NPNAx5 was consistently found to be optimal, NPNAx20 showed the best protection upon rechallenge.

Nonhuman Primate Studies Confirmed the Superior Immunogenicity of TMV-NPNAx5. To determine if vaccine responses were translatable to humans, we next compared the TMV and FL-CSP vaccine in two nonhuman primate (NHP) models. Indian-origin

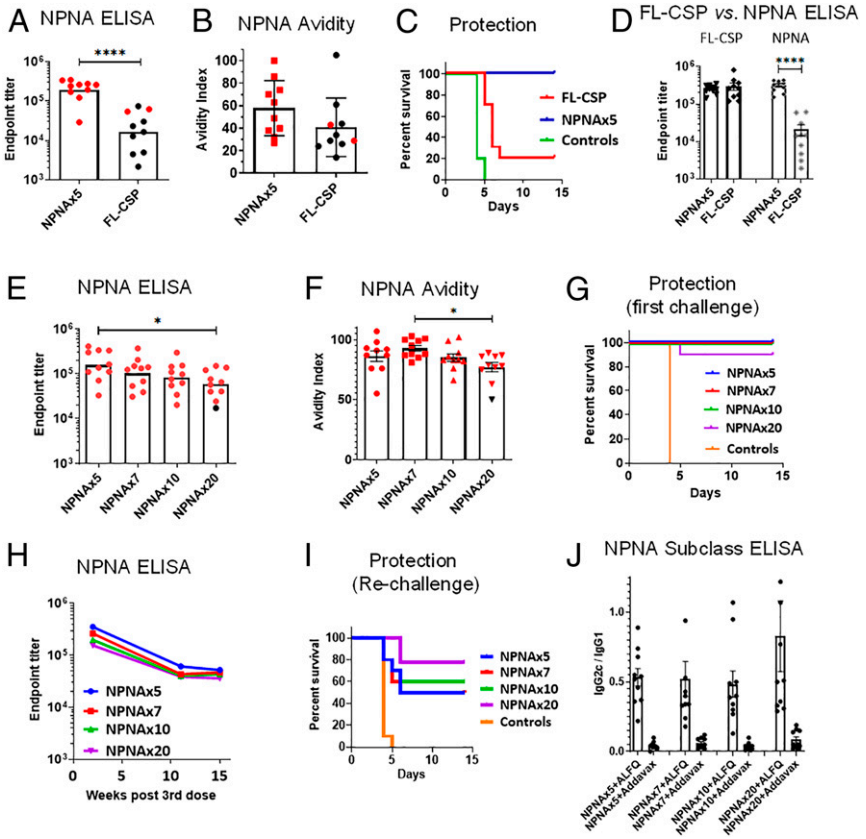

Fig. 5. TMV-NPNAx5/ALFQ immunogenicity in C57BL/6 mouse challenge model. Mice ($n = 10$) were immunized 3× 2.5 μg dose of NPNAx5, FL-CSP in ALFQ (*A–D*) or with 3× 2.5 μg dose of NPNAx5, -x7, -x10, and -x20 vaccines in ALFQ (*E–J*). At 2 wk after the third dose, ELISA was conducted and mice were challenged. (*A* and *E*) Geometric mean NPNA titers. (*B* and *F*) Mean avidity index using repeat peptide coat. (*C* and *G*) Survival curve of mice following challenge. (*D*) Relative titers against FL-CSP and repeat peptide coat for NPNAx5/ALFQ and FL-CSP/ALFQ vaccinated mice. (*H*) The mice that survived the challenge were bled again at week 11 and week 15 and their repeat ELISA titers were plotted. (*I*) Results of rechallenge of mice at 15 wk after the third dose. (*J*) Subclass analysis of mice by ELISA showing the ratio of IgG2c: IgG1 titer. Error bars are ±SEM; red symbols are protected mice; ****$P < 0.0001$; *$P < 0.05$.

rhesus macaques were vaccinated three times with 20 or 40 μg TMV-NPNAx5 compared to 40 μg FL-CSP in ALFQ adjuvant. No signs of vaccine-related adverse events were noted. Repeat-specific titers after the first dose were similar, but the second and third vaccination with TMV-NPNAx5 boosted repeat titers better than FL-CSP. At 2 wk after the third dose, titer in the 40-μg TMV-NPNAx5 group was fivefold higher than FL-CSP, with both TMV-NPNAx5 groups showing >100,000 titer (Fig. 6*A* and *SI Appendix*, Fig. S6*F*) and the avidity index was >60% (Fig. 6*B*). Sera had to be diluted 1:200 to discern differences between ILSDA activities between groups. At this serum dilution, >90% mean ILSDA activity was observed in both TMV-NPNAx5 groups compared to <60% ILSDA for FL-CSP group (Fig. 6*C*). All of the above immunological readouts were statistically significant in favor of the TMV-NPNAx5 vaccine groups.

Similar to mice, rhesus showed a biphasic decay of Abs after the third dose; a fast drop was followed by plateauing of titers (compare Fig. 6*D* and Fig. 5*H*). The TMV-NPNAx5 group titers remained significantly above FL-CSP until ∼20 wk after the third dose (two-way ANOVA followed by Tukey's correction). The functionality of pooled sera, diluted 1:80, was assessed by ILSDA. As expected at 4 wk after the third dose all vaccine groups showed >90% ILSDA activity. However, after 12 wk, anti–FL-CSP ILSDA activity rapidly dropped to <70%, while the two TMV-NPNAx5 vaccine groups showed a much slower drop in ILSDA activity. The low-dose 20-μg TMV-NPNAx5 group titers plateaued at >10,000 and these Abs continued to show >80% ILSDA activity up to the 47 wk after the third dose time point examined (Fig. 6*E*). This high level of parasite inhibitory activity was also confirmed using ILSDA on sera from individual monkeys (*SI Appendix*, Fig. S8).

In a subsequent rhesus study, 40 μg TMV-NPNAx5 ($n = 6$), 40 μg TMV-NPNAx20 ($n = 4$), or 40 μg FL-CSP ($n = 6$) formulated in ALFQ were compared in Chinese-origin rhesus macaques (Fig. 6 *F–H*). Three doses of the vaccine were given 4 wk apart. Compared to the FL-CSP titer at 2 wk after the third dose, the repeat titers of TMV-NPNAx5 was 2.3× higher and that of TMV-NPNAx20 was 1.6× higher (*SI Appendix*, Fig. S6*G*). There was no difference between the titer of TMV-NPNAx5 and TMV-NPNAx20 groups (Fig. 6*F*). Unlike the results in Indian rhesus, the avidity difference between FL-CSP and TMV vaccines was not statistically significant in Chinese rhesus (Fig. 6*G*). However, ILSDA activity at 1:300 serum dilution showed a clear superiority of the TMV vaccines over FL-CSP (Fig. 6*H*). The data confirmed the equivalence of NPNAx5 and NPNAx20 vaccines and superiority over FL-CSP in the rhesus model.

ELISA and avidity assays for rhesus sera were performed by the International Malaria Serology Reference Center using a standardized human repeat ELISA. The same assay was used to report the immunological end-points for RTS,S/AS01 as part of the MAL071 clinical trial (28). While a direct comparison of ELISA between rhesus and humans can be confounded by cross-reactivity differences in secondary Abs, the geometric mean of titer and mean avidity index for the standard dose of RTS,S/AS01 was shown as a red line to provide context to the

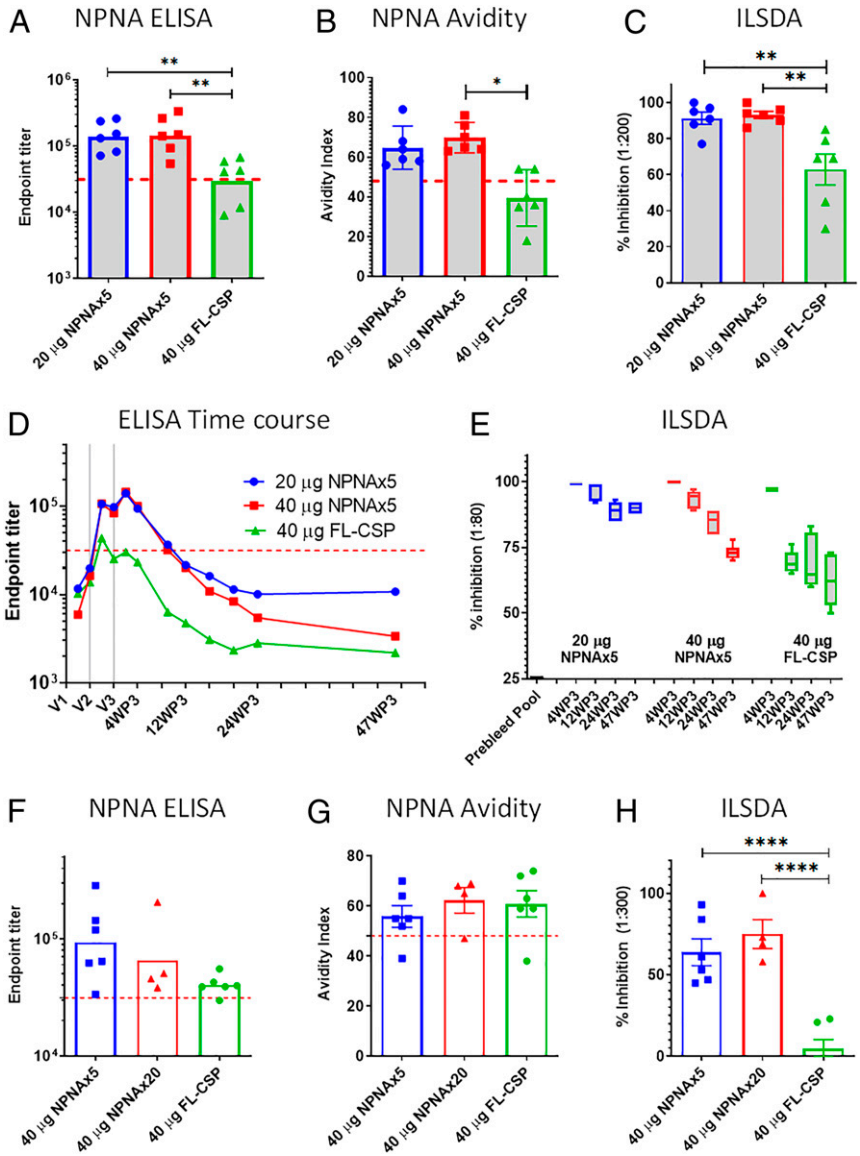

Fig. 6. Rhesus model immunogenicity. (*A–E*) Rhesus of Indian origin ($n = 6$) vaccinated three times with 20 μg or 40 μg NPNAx5 or 40 μg FL-CSP in ALFQ adjuvant. (*F–H*) Rhesus of Chinese origin vaccinated thrice with 40 μg of NPNAx5 ($n = 6$), 40 μg NPNAx20 ($n = 4$), or 40 μg FL-CSP ($n = 6$) in ALFQ. (*A* and *F*) Geometric mean ELISA titer at 2 wk after the third dose; (*B* and *G*) Mean repeat peptide avidity index; (*C* and *H*) Mean ILSDA at 1:200 or 1:300 serum dilution. (*D*) Repeat Ab geometric mean titer over 47 wk after the third dose; the time of each vaccination is marked as V1, V2, V3. The 47WP3 time-point has data from a subset of animals; 20 μg NPNAx5 ($n = 3$); both 40-μg dose groups ($n = 2$ each). Dotted line indicates historical geometrical mean values at 3 wk after the dose in RTS,S/AS01 vaccinated humans vaccinated on a 0- to 1–2-mo schedule (28). (*E*) ILSDA assay at 1:80 pooled serum dilution at four time-points weeks 4, 12, 24, and 47 after the third dose. $^{****}P < 0.0001$; $^{**}P < 0.01$.

nonhuman primate data reported here for the NPNAx5 vaccine (Fig. 6 *A–G*).

Discussion

Mathematical modeling reveals that the high antigenic complexity of CSP negatively impacts efficient affinity maturation of B cells (34, 57). The 10× higher titer and higher avidity in mice of TMV-NPNAx5 displayed on a loop, compared to the FL-CSP and N- and C-terminally tethered NPNAx5, could be the result of reduced antigen complexity due to the diminished antigen flexibility. Furthermore, 17 monomers of TMV capsid displayed ∼85 NPNA repeats per NPNAx5 disk, potentially augmenting B cell cross-linking by particulate display (42, 58). The greater longevity of the low-dose TMV-NPNAx5 group in the rhesus experiment is also possible evidence of further augmentation of the B cell response through lower antigen dosing (Fig. 6*D*). Upon increasing the loop size from NPNAx3 to NPNAx5, antibody avidity was unchanged but the titer increased. The shorter NPNAx3 loop may be overly restricted, which is consistent with the low potency of mAbs 580 and CIS43 binding. Interestingly, there was no significant improvement of vaccine performance between NPNAx5 and NPNAx20 in mice or rhesus, and there was evidence to indicate that NPNAx20 antibodies had lower titer and avidity compared to NPNAx5 group in mice. It is possible that at NPNA copy number around 20, increases the proportion of B cells that undergo apoptosis due to hypercross-linking (59–61). Overall in the mouse model, the NPNAx5 antigen displayed on a loop consistently showed optimal immunogenicity and presumably represented a balance between flexibility and copy number.

Across *Plasmodium* species, CSP repeat sequences allow the formation of short structured motifs within a flexible repeat

region (40, 62). For example, proline and alanine within the poly-NPNA have low side-chain entropy and the asparagine residue can hydrogen-bond with the peptide back-bone. *Plasmodium vivax* CSP repeats, GNQPGANGA or GQPAGDRA(A/D), also contain residues with low side-chain entropy (glycine, proline, and alanine) and residues that hydrogen bond to the main chain (glutamine, asparagine, and aspartate). The partially constrained structural flexibility of the CSP repeats may be an escape mechanism, activating a diverse repertoire of B cells, only a fraction of which develop into plasma cells that produce high affinity and functional antibodies. The structure of RTS,S is not known, but it contains 19 NANP repeats expressed as an N-terminal fusion to the hepatitis B particle, and while optimal copy number may vary between display platforms (25, 27), our results suggest that lowering repeat copy number and looped presentation may improve immunogenicity and protection of the current vaccine.

Vaccine design screening studies using in vivo immunogenicity and protection readouts can require a large number of animals. An in vitro screen using a panel of well-characterized mAbs could greatly facilitate this effort (63). The positive association of mAb 580 potency with copy number prompted us to hypothesize that diminished abundance of low-affinity epitopes in a vaccine could translate to elicitation of polyclonal antibodies of higher average avidity. However, this was not the case with TMV-NPNAx3, which showed a higher proportion of constrained conformation antibodies, but the mouse titers were suboptimal and avidity did not differ from NPNAx5. mAbs CIS43 or 580 potency for TMV-NPNAx3 was poor, suggesting a lack of the minimal protective epitope displayed, and poor mAb 580 potency could be due to the inability of the NPNAx3 loop to sustain cross-linking of a low-affinity antibody via homotypic interactions (57, 64) or additive binding (65). TMV-NPNAx5 may also reflect the right balance between limiting low-affinity mAb epitope abundance and efficient binding to high-affinity CSP mAbs. It is possible that an excess of mAb 580 binding epitopes in NPNAx20 or FL-CSP as compared to NPNAx5, could have resulted in lower-avidity polyclonal antibodies observed in mice. Furthermore, the potency of mAb 580 for TMV-CT was threefold better than for TMV-Loop and the avidity of TMV-CT Abs was also lower than TMV-Loop, but no different from FL-CSP Abs. Taken together, these data give us a glimpse at potency of mAb binding positively or negatively predicting immunogenicity outcomes for CSP vaccines. A future study using a panel of neutralizing and nonneutralizing antibodies can downselect mAbs that definitively predict CSP vaccine outcomes. Access to RTS,S and sera from protected/nonprotected volunteers could greatly facilitate the development of more precise assays to screen for improved CSP vaccines, similar to those that led to improving the RSV vaccine (66).

FL-CSP contains 19 copies of NPNA and yet the most striking discordance between high mAb potency and low vaccine performance was that for FL-CSP. One reason could be that FL-CSP contains competing epitopes from the flanking N- and C-terminal regions of CSP. The 277-amino acid long FL-CSP vaccination induces antibodies against epitopes spread all across the CSP molecule (43). In contrast, the TMV response was highly focused to a 20-amino acid target (Fig. 5*D*). Repeat Ab titers and avidity has been associated with protection (28, 67), but several studies show C-terminal mAbs have little neutralizing activity (4). Although polymorphisms within the C-terminal region were implicated in escape from RTS,S-mediated protection (6), our data showed no discernable antiparasitic effects of C-terminal Abs despite their high avidity (*SI Appendix*, Fig. S3). Nonfunctional B cell epitopes in vaccines could compete for immunological space during the Ab induction and maturation phases (68) and nonfunctional Abs can sterically block functional Abs from binding to the target (69). Our results, and clinical experience with repeatless CSP vaccines (70), argue that a repeat-only, particulate CSP vaccine, combined with a molecular adjuvant like AS01/ALFQ, needs to be assessed in humans.

A flat TMV disk could be sterically less restrictive than VLPs that require sphere closure. Up to an 80-amino acid insert (NPNAx20) was successfully displayed on TMV, but only a 20-amino acid insert (NPNAx5) may be required to protect against *P. falciparum*, thus leaving potential space within the TMV particle for additional vaccine epitopes, such as the junctional epitope (30, 31) or the repeat region of *P. vivax* CSP. Expression and purification of TMV was accomplished here in *E. coli*; however, an optimized TMV-based malaria vaccine could also be manufactured *in planta*.

A 10× improvement in repeat titers for TMV-NPNAx5 over FL-CSP was observed in mice but protection in a rechallenge study was better for TMV-NPNAx20. In rhesus of Indian origin, TMV-NPNAX5 showed a 5× improvement in titer over FL-CSP but rhesus of Chinese origin showed a 2.3× difference. Unlike mice, the Chinese origin rhesus showed no difference between TMV-NPNAx5 and TMV-NPNAx20 vaccines, confirming our long-standing position that immunological comparison in rhesus remain on critical path prior to advancing second generation vaccine candidates to humans (44, 71, 72). TMV-NPNAx5/ALFQ antibodies in rhesus macaques inhibited sporozoite invasion for up to a year, leading us to hypothesize that an optimized epitope-based vaccine could protect against malaria for up to a year and may be sustained thereafter by an annual booster vaccination. Based on the evidence provided here, TMV-NPNAx5 and TMV-NPNAx20 can be considered as candidates for testing the first TMV-based vaccine in humans.

ACKNOWLEDGMENTS. We thank Colonel Viseth Ngauy, Chief Malaria Vaccine Branch, Walter Reed Army Institute of Research (WRAIR) for critically reviewing the manuscript, providing input on monoclonal anitibody development, and tobacco mosaic virus product development; Dr. Robert Schwenk, Retired Scientist, Malaria Vaccine Branch for manuscript review and expert advice; Dr. Evelina Angov for facilitating the clinical development of ALFQ adjuvant; Leutenant Colonel Tony Pierson and Dr. Elke Bergmann-Leitner at the WRAIR International Reference Serology Laboratory and the Flow Cytometric Center for providing the repeat human peptide ELISA data on the rhesus sera; Mr. Edward Asafo Adjei at the WRAIR Division of Pathology, for electron microscopy support; the staff at the WRAIR Veterinary Medicine Branch, for help with animal handling; the WRAIR Division of Entomology, for maintaining and providing the transgenic parasites needed to infect mosquitoes; Drs. Roberta Spaccapelo, Università degli Studi di Perugia, and Andrea Crisanti, Imperial College London, for providing the transgenic strain parasites; and Drs. Lorraine Soisson, Robin Miller, and Carter Diggs, Malaria Vaccine Development Program US Agency for International Development (USAID) for their advice and guidance. Funding for this work was provided by the US Department of Defense and by the USAID Malaria Vaccine Program through an Interagency Agreement. Material has been reviewed by WRAIR and the USAID. There is no objection to its presentation and/or publication. The opinions or assertions contained herein are the private views of the author, and are not to be construed as official, or as reflecting true views of the Department of the Army, the Department of Defense, or the USAID.

1. World Health Organiztion, *World Malaria Report 2018* (WHO, Geneva, 2018).
2. N. M. Bowman *et al*., Comparative population structure of Plasmodium falciparum circumsporozoite protein NANP repeat lengths in Lilongwe, Malawi. *Sci. Rep.* **3**, 1990 (2013).
3. M. J. Lockyer, R. T. Schwarz, Strain variation in the circumsporozoite protein gene of Plasmodium falciparum. *Mol. Biochem. Parasitol.* **22**, 101–108 (1987).
4. S. W. Scally *et al*., Rare PfCSP C-terminal antibodies induced by live sporozoite vaccination are ineffective against malaria infection. *J. Exp. Med.* **215**, 63–75 (2018).
5. R. Herrera *et al*., Reversible conformational change in the Plasmodium falciparum circumsporozoite protein masks its adhesion domains. *Infect. Immun.* **83**, 3771–3780 (2015).
6. D. E. Neafsey *et al*., Genetic diversity and protective efficacy of the RTS,S/AS01 malaria vaccine. *N. Engl. J. Med.* **373**, 2025–2037 (2015).
7. D. A. Espinosa *et al*., Proteolytic cleavage of the Plasmodium falciparum circumsporozoite protein is a target of protective antibodies. *J. Infect. Dis.* **212**, 1111–1119 (2015).

8. K. E. Kester *et al*., RTS,S Vaccine Evaluation Group, Randomized, double-blind, phase 2a trial of falciparum malaria vaccines RTS,S/AS01B and RTS,S/AS02A in malaria-naive adults: Safety, efficacy, and immunologic associates of protection. *J. Infect. Dis.* **200**, 337–346 (2009).
9. J. A. Stoute *et al*., A preliminary evaluation of a recombinant circumsporozoite protein vaccine against Plasmodium falciparum malaria. RTS,S Malaria Vaccine Evaluation Group. *N. Engl. J. Med.* **336**, 86–91 (1997).
10. G. Leroux-Roels *et al*., Evaluation of the immune response to RTS,S/AS01 and RTS,S/AS02 adjuvanted vaccines: Randomized, double-blind study in malaria-naïve adults. *Hum. Vaccin. Immunother.* **10**, 2211–2219 (2014).
11. S. T. Agnandji *et al*.; RTS,S Clinical Trials Partnership, First results of phase 3 trial of RTS,S/AS01 malaria vaccine in African children. *N. Engl. J. Med.* **365**, 1863–1875 (2011).
12. P. A. Minsoko *et al*.; RTS,S Clinical Trials Partnership, Efficacy and safety of the RTS,S/AS01 malaria vaccine during 18 months after vaccination: A phase 3 randomized, controlled trial in children and young infants at 11 African sites. *PLoS Med.* **11**, e1001685 (2014).
13. S. T. Agnandji *et al*.; RTS,S Clinical Trials Partnership, A phase 3 trial of RTS,S/AS01 malaria vaccine in African infants. *N. Engl. J. Med.* **367**, 2284–2295 (2012).
14. D. M. Gordon *et al*., Safety, immunogenicity, and efficacy of a recombinantly produced Plasmodium falciparum circumsporozoite protein-hepatitis B surface antigen subunit vaccine. *J. Infect. Dis.* **171**, 1576–1585 (1995).
15. R. Schwenk *et al*., IgG2 antibodies against a clinical grade Plasmodium falciparum CSP vaccine antigen associate with protection against transgenic sporozoite challenge in mice. *PLoS One* **9**, e111020 (2014).
16. A. R. Noe *et al*., A full-length Plasmodium falciparum recombinant circumsporozoite protein expressed by Pseudomonas fluorescens platform as a malaria vaccine candidate. *PLoS One* **9**, e107764 (2014).
17. F. Amelia *et al*., Down-selecting circumsporozoite protein-based malaria vaccine: A comparison of malaria sporozoite challenge model. *Parasite Immunol.* **41**, e12624 (2019).
18. K. A. Collins, R. Snaith, M. G. Cottingham, S. C. Gilbert, A. V. S. Hill, Enhancing protective immunity to malaria with a highly immunogenic virus-like particle vaccine. *Sci. Rep.* **7**, 46621 (2017).
19. A. Birkett *et al*., A modified hepatitis B virus core particle containing multiple epitopes of the Plasmodium falciparum circumsporozoite protein provides a highly immunogenic malaria vaccine in preclinical analyses in rodent and primate hosts. *Infect. Immun.* **70**, 6860–6870 (2002).
20. E. H. Nardin *et al*., A totally synthetic polyoxime malaria vaccine containing Plasmodium falciparum B cell and universal T cell epitopes elicits immune responses in volunteers of diverse HLA types. *J. Immunol.* **166**, 481–489 (2001).
21. S. A. Kaba *et al*., Protective antibody and CD8+ T-cell responses to the Plasmodium falciparum circumsporozoite protein induced by a nanoparticle vaccine. *PLoS One* **7**, e48304 (2012).
22. C. Palma *et al*., Adenovirus particles that display the Plasmodium falciparum circumsporozoite protein NANP repeat induce sporozoite-neutralizing antibodies in mice. *Vaccine* **29**, 1683–1689 (2011).
23. M. Iyori *et al*., Protective efficacy of baculovirus dual expression system vaccine expressing Plasmodium falciparum circumsporozoite protein. *PLoS One* **8**, e70819 (2013).
24. C. M. Janitzek *et al*., Bacterial superglue generates a full-length circumsporozoite protein virus-like particle vaccine capable of inducing high and durable antibody responses. *Malar. J.* **15**, 545 (2016).
25. A. Urakami *et al*., Development of a novel virus-like particle vaccine platform that mimics the immature form of alphavirus. *Clin. Vaccine Immunol.* **24**, e00090-17 (2017).
26. D. C. Whitacre *et al*., P. falciparum and P. vivax epitope-focused VLPs elicit sterile immunity to blood stage infections. *PLoS One* **10**, e0124856 (2015).
27. N. J. Kingston *et al*., Hepatitis B virus-like particles expressing Plasmodium falciparum epitopes induce complement-fixing antibodies against the circumsporozoite protein. *Vaccine* **37**, 1674–1684 (2019).
28. J. A. Regules *et al*., Fractional third and fourth dose of RTS,S/AS01 malaria candidate vaccine: A phase 2a controlled human malaria parasite infection and immunogenicity study. *J. Infect. Dis.* **214**, 762–771 (2016).
29. D. Oyen *et al*., Structural basis for antibody recognition of the NANP repeats in *Plasmodium falciparum* circumsporozoite protein. *Proc. Natl. Acad. Sci. U.S.A.* **114**, E10438–E10445 (2017). Erratum in: *Proc. Natl. Acad. Sci. U.S.A.* **115**, E5838–E5839 (2018).
30. J. Tan *et al*., A public antibody lineage that potently inhibits malaria infection through dual binding to the circumsporozoite protein. *Nat. Med.* **24**, 401–407 (2018).
31. N. K. Kisalu *et al*., A human monoclonal antibody prevents malaria infection by targeting a new site of vulnerability on the parasite. *Nat. Med.* **24**, 408–416 (2018).
32. G. M. Bartelds *et al*., Development of antidrug antibodies against adalimumab and association with disease activity and treatment failure during long-term follow-up. *J. Am. Med. Assoc.* **305**, 1460–1468 (2011).
33. H. Morgan *et al*., Evaluation of in vitro assays to assess the modulation of dendritic cells functions by therapeutic antibodies and aggregates. *Front. Immunol.* **10**, 601 (2019).
34. H. Wardemann, R. Murugan, From human antibody structure and function towards the design of a novel Plasmodium falciparum circumsporozoite protein malaria vaccine. *Curr. Opin. Immunol.* **53**, 119–123 (2018).
35. G. Triller *et al*., Natural parasite exposure induces protective human anti-malarial antibodies. *Immunity* **47**, 1197–1209.e10 (2017).
36. A. M. Killikelly, M. Kanekiyo, B. S. Graham, Pre-fusion F is absent on the surface of formalin-inactivated respiratory syncytial virus. *Sci. Rep.* **6**, 34108 (2016).
37. M. C. Crank *et al*.; VRC 317 Study Team, A proof of concept for structure-based vaccine design targeting RSV in humans. *Science* **365**, 505–509 (2019).
38. C. A. MacRaild *et al*., Conformational dynamics and antigenicity in the disordered malaria antigen merozoite surface protein 2. *PLoS One* **10**, e0119899 (2015).
39. A. Ghasparian, K. Moehle, A. Linden, J. A. Robinson, Crystal structure of an NPNA-repeat motif from the circumsporozoite protein of the malaria parasite Plasmodium falciparum. *Chem. Commun. (Camb.)*, 174–176 (2006).
40. H. J. Dyson, A. C. Satterthwait, R. A. Lerner, P. E. Wright, Conformational preferences of synthetic peptides derived from the immunodominant site of the circumsporozoite protein of Plasmodium falciparum by 1H NMR. *Biochemistry* **29**, 7828–7837 (1990).
41. T. V. Gasanova, N. V. Petukhova, P. A. Ivanov, Chimeric particles of tobacco mosaic virus as a platform for the development of next-generation nanovaccines. *Nanotechnol. Russ.* **11**, 227–236 (2016).
42. L. Zhao *et al*., Nanoparticle vaccines. *Vaccine* **32**, 327–337 (2014).
43. C. J. Genito *et al*., Liposomes containing monophosphoryl lipid A and QS-21 serve as an effective adjuvant for soluble circumsporozoite protein malaria vaccine FMP013. *Vaccine* **35**, 3865–3874 (2017).
44. A. Cawlfield *et al*., Safety, toxicity and immunogenicity of a malaria vaccine based on the circumsporozoite protein (FMP013) with the adjuvant army liposome formulation containing QS21 (ALFQ). *Vaccine* **37**, 3793–3803 (2019).
45. R. Tewari, R. Spaccapelo, F. Bistoni, A. A. Holder, A. Crisanti, Function of region I and II adhesive motifs of Plasmodium falciparum circumsporozoite protein in sporozoite motility and infectivity. *J. Biol. Chem.* **277**, 47613–47618 (2002).
46. M. D. Porter *et al*., Transgenic parasites stably expressing full-length Plasmodium falciparum circumsporozoite protein as a model for vaccine down-selection in mice using sterile protection as an endpoint. *Clin. Vaccine Immunol.* **20**, 803–810 (2013).
47. X. Zou, B. L. House, M. D. Zyzak, T. L. Richie, V. R. Gerbasi, Towards an optimized inhibition of liver stage development assay (ILSDA) for Plasmodium falciparum. *Malar. J.* **12**, 394 (2013).
48. National Research Council, *Guide for the Care and Use of Laboratory Animals* (National Academies Press, Washington, DC, ed. 8, 2011).
49. J. Röder, R. Fischer, U. Commandeur, Adoption of the 2A ribosomal skip principle to Tobacco Mosaic Virus for peptide display. *Front. Plant Sci.* **8**, 1125 (2017).
50. R. C. McComb, C. L. Ho, K. A. Bradley, L. K. Grill, M. Martchenko, Presentation of peptides from Bacillus anthracis protective antigen on Tobacco Mosaic Virus as an epitope targeted anthrax vaccine. *Vaccine* **33**, 6745–6751 (2015).
51. N. V. Petukhova, T. V. Gasanova, P. A. Ivanov, J. G. Atabekov, High-level systemic expression of conserved influenza epitope in plants on the surface of rod-shaped chimeric particles. *Viruses* **6**, 1789–1800 (2014).
52. A. A. McCormick, K. E. Palmer, Genetically engineered tobacco mosaic virus as nanoparticle vaccines. *Expert Rev. Vaccines* **7**, 33–41 (2008).
53. M. T. Dedeo, K. E. Duderstadt, J. M. Berger, M. B. Francis, Nanoscale protein assemblies from a circular permutant of the tobacco mosaic virus. *Nano Lett.* **10**, 181–186 (2010).
54. Y. Song *et al*., High-resolution comparative modeling with RosettaCM. *Structure* **21**, 1735–1742 (2013).
55. S. Raman *et al*., Structure prediction for CASP8 with all-atom refinement using Rosetta. *Proteins* **77** (suppl. 9), 89–99 (2009).
56. F. Zavala, A. H. Cochrane, E. H. Nardin, R. S. Nussenzweig, V. Nussenzweig, Circumsporozoite proteins of malaria parasites contain a single immunodominant region with two or more identical epitopes. *J. Exp. Med.* **157**, 1947–1957 (1983).
57. R. Murugan *et al*., Clonal selection drives protective memory B cell responses in controlled human malaria infection. *Sci. Immunol.* **3**, eaap8029 (2018).
58. M. F. Bachmann, G. T. Jennings, Vaccine delivery: A matter of size, geometry, kinetics and molecular patterns. *Nat. Rev. Immunol.* **10**, 787–796 (2010).
59. Q. Qin, Z. Yin, X. Wu, K. M. Haas, X. Huang, Valency and density matter: Deciphering impacts of immunogen structures on immune responses against a tumor associated carbohydrate antigen using synthetic glycopolymers. *Biomaterials* **101**, 189–198 (2016).
60. S. L. Parry, J. Hasbold, M. Holman, G. G. Klaus, Hypercross-linking surface IgM or IgD receptors on mature B cells induces apoptosis that is reversed by costimulation with IL-4 and anti-CD40. *J. Immunol.* **152**, 2821–2829 (1994).
61. M. Mayumi *et al*., IgM-mediated B cell apoptosis. *Crit. Rev. Immunol.* **15**, 255–269 (1995).
62. T. E. Lehmann *et al*., Plasmodium vivax CS peptides display conformational preferences for folded forms in solution. *J. Pept. Res.* **61**, 252–262 (2003).
63. B. S. Graham, M. S. A. Gilman, J. S. McLellan, Structure-based vaccine antigen design. *Annu. Rev. Med.* **70**, 91–104 (2019).
64. D. Oyen *et al*., Cryo-EM structure of P. falciparum circumsporozoite protein with a vaccine-elicited antibody is stabilized by somatically mutated inter-Fab contacts. *Sci. Adv.* **4**, eaau8529 (2018).
65. C. R. Fisher *et al*., T-dependent B cell responses to Plasmodium induce antibodies that form a high-avidity multivalent complex with the circumsporozoite protein. *PLoS Pathog.* **13**, e1006469 (2017).
66. E. Phung *et al*., Epitope-specific serological assays for RSV: Conformation matters. *Vaccines (Basel)* **7**, E23 (2019).
67. M. T. White *et al*., The relationship between RTS,S vaccine-induced antibodies, $CD4^+$ T cell responses and protection against Plasmodium falciparum infection. *PLoS One* **8**, e61395 (2013).
68. S. Chaudhury, J. Reifman, A. Wallqvist, Simulation of B cell affinity maturation explains enhanced antibody cross-reactivity induced by the polyvalent malaria vaccine AMA1. *J. Immunol.* **193**, 2073–2086 (2014).
69. C. Uthaipibull *et al*., Inhibitory and blocking monoclonal antibody epitopes on merozoite surface protein 1 of the malaria parasite Plasmodium falciparum. *J. Mol. Biol.* **307**, 1381–1394 (2001).
70. D. G. Heppner *et al*., Safety, immunogenicity, and efficacy of Plasmodium falciparum repeatless circumsporozoite protein vaccine encapsulated in liposomes. *J. Infect. Dis.* **174**, 361–366 (1996).
71. T. W. Phares *et al*., Rhesus macaque and mouse models for down-selecting circumsporozoite protein based malaria vaccines differ significantly in immunogenicity and functional outcomes. *Malar. J.* **16**, 115 (2017).
72. M. L. Martin *et al*., Comparison of immunogenicity and safety outcomes of a malaria vaccine FMP013/ALFQ in rhesus macaques (Macaca mulatta) of Indian and Chinese origin. *Malar. J.* **18**, 377 (2019).